AN EULERIAN FINITE VOLUME METHOD FOR HYDRAULIC FRACTURE PROBLEMS

ANTHONY P. PEIRCE* AND EDUARD SIEBRITS†

Abstract. Hydraulic fracturing is a process that is often used in the oil and gas industry to enhance the flow of hydrocarbons by generating a fracture within a reservoir. The fracture is propagated by injecting a viscous fluid into a bore-hole under a sufficiently high pressure to overcome the tensile strength of the rock and the ambient geological stresses. We describe an Eulerian Finite Volume scheme based on a fixed rectangular grid to solve the coupled system of hydraulic fracture nonlinear integro-partial differential equations. We illustrate the accuracy of the algorithm by comparing the Finite Volume solution to the exact solution for a radial solution evolving in a homogeneous elastic medium.

Key words. Finite Volume Methods, fluid driven fractures, hydraulic fracture, boundary integral methods.

1. Introduction. Hydraulic fracturing is a process by which a fracture is propagated in brittle rock by injecting a viscous fluid into a perforated section of a bore-hole under a sufficiently high pressure to overcome the tensile strength of the rock and the minimum principal geological stresses. As a result, a fracture surface, which is often assumed to be planar, develops in a direction perpendicular to this minimum principal stress. Hydraulic fracturing is frequently used in the oil and gas recovery industry to induce fractures in reservoirs in order to substantially enhance the flow of hydrocarbons. The process has also been used in the mining industry to introduce large fractures in the rock surrounding mining excavations in order to enlarge these excavations without having to use explosive charges. Environmental engineers have also used hydraulic fracturing to isolate toxic substances by injecting impermeable materials into fractures. In all these processes, it is desirable to be able to predict the evolution of the fracture surface under known stress and geological conditions. Thus robust, efficient, and accurate numerical modeling of hydraulically driven fractures is of considerable interest.

The governing equations that describe the evolution of a hydraulic fracture involve: the two-dimensional (2D) Reynold's lubrication equation expressing the conservation of fluid volume within the planar fracture; the three-dimensional (3D) equilibrium and elastic stress-strain partial differential equations that in this case can be reduced to a (2D) boundary integral equation expressing the balance of forces between the fluid pressure, the geological stresses, and the elastic response of the reservoir; and a propagation criterion which determines the extent of the fracture footprint. Some previous algorithms to solve this problem (see [2], [3]) have used a Lagrangian Finite Element formulation in which a mapped moving mesh is used to model the arbitrarily shaped fracture as it evolves. However, for each fracture footprint in such a model, the fully populated Green's function influence matrix has to be constructed, which for an inhomogeneous or even a layered elastic medium can be an extremely time consuming process. In order to avoid the computational expense of having to construct the Green's function matrix for the elasticity integral equation at each time-step, we adopt an Eulerian approach in which the fracture is considered to evolve within a pre-defined rectangular grid. In this paper we describe a Finite Volume algorithm to model the evolution of an arbitrarily shaped planar hydraulic fracture within a 3D

*University of British Columbia, Vancouver, Canada, peirce@math.ubc.ca
†Schlumberger Technology Corporation, Sugar Land, TX, USA.

elastic medium. Using this grid structure, the interior of the fracture can be modeled by rectangular elements, while those elements that intersect with the fracture front are broken into polygonal sub-regions. For the fluid flow equations we use the Cartesian Finite Volume formulation introduced by Calhoun and Le Veque [1]. The integral equation is accurately approximated in this context by using a partially filled element concept introduced by Ryder and Napier [6]. These two schemes are combined to solve the coupled fluid-flow partial differential and elasticity integral equations that describe the hydraulic fracture process.

In section 2 we describe the continuous coupled integro-partial differential equations that govern the evolution of a fluid-driven fracture. In section 3, we describe the discretization procedure used to solve the governing equations. In section 4, we present results on the performance of the Finite Volume algorithm. In section 5 we make some concluding remarks.

2. Governing equations. In a 3D layered elastic medium the integral equation governing the width profile for a planar crack can be written in the form:

$$\int\limits_{\Omega(t)} C(x,y;\xi,\eta)w(\xi,\eta,t)d\xi d\eta = p(x,y,t) - \sigma_c(x,y) \tag{2.1}$$

where the fracture is subjected to a fluid pressure $p(x,y,t)$ that works against the far-field minimum principal stress field $\sigma_c(x,y)$ within the elastic medium. If p is sufficiently large to overcome σ_c then the fracture opens by an amount $w(\xi,\eta,t)$. The Green's function $C(x,y;\xi,\eta)$ contains all the information about the stiffness of the layered elastic medium. The fracture at time t is assumed to occupy the region denoted by $\Omega(t)$, which has a boundary that we denote by $\partial\Omega$.

In the case of a planar fracture that grows in a 3D elastic medium, the fluid flow equations are well approximated by the 2D Reynold's lubrication equation:

$$\frac{\partial w}{\partial t} = \bigtriangledown \bullet (D(w) \bigtriangledown p) + \delta(x,y)Q \text{ and } D(w)\frac{\partial p}{\partial n} \mid_{\partial\Omega} = 0 \tag{2.2}$$

where $Q = Q(x,y,t)$ is the volume of fluid pumped into the fracture at the well bore. For simplicity, we have assumed no leakoff of fluid to the elastic medium and that the fluid is Newtonian so that $D(w) = \frac{w^3}{12\mu}$, where μ is the fluid viscosity. For a non-Newtonian power-law fluid $D(w)$ is replaced by $D(w, |\nabla p|)$ in which the dependence of D on w is larger than a cubic power while D has a power-law dependence on $|\nabla p|$ in which the exponent is positive.

3. Discretization of the governing equations.

3.1. Finite Volume discretization of the fluid flow equations. We assume that the fracture region $\Omega(t)$ evolves in a window that has been divided into rectangular elements. We make use of the Finite Volume method for discretizing the fluid flow equations on this rectangular Eulerian grid (see [1]) which is broken into polygonal elements to describe the tip of the arbitrarily shaped fracture. Similar to the Finite Element Method this method automatically builds in the zero flux natural boundary condition of the form $D(w)dp/dn = 0$ along the piecewise linear portions of the fracture front.

Integrating (2.2) over an element Ω_e, which is a rectangle of size $\Delta x \Delta y$ for interior elements or a polygon in the case of tip elements (see figure 3.1) and applying Green's

theorem results in:

$$\frac{\partial}{\partial t}\int_{\Omega_e} K w dx dy = \int_{\partial\Omega_e} D(w)\frac{\partial p}{\partial n} dS + Q$$

where $K(x,y)$ is a "capacity" function that we will use to represent a fill fraction. In the above integrated equation, we infer that Q is only non-zero for source elements. Discretization on an interior rectangular element centered at (i,j) yields:

$$K_{i,j}\Delta x\Delta y\left(\frac{w_{i,j}-(w_{old})_{i,j}}{\Delta t}\right) = \Delta y(F_{i+1/2,j}-F_{i-1/2,j})+ \\ \Delta x(F_{i,j+1/2}-F_{i,j-1/2}) + Q_{i,j}$$

where

$$F_{i+1/2,j} = D_{i+1/2,j}\left(\frac{p_{i+1,j}-p_{i,j}}{\Delta x}\right) \text{ and } F_{i-1/2,j} = D_{i-1/2,j}\left(\frac{p_{i,j}-p_{i-1,j}}{\Delta x}\right)$$

$$F_{i,j+1/2} = D_{i,j-1/2}\left(\frac{p_{i,j+1}-p_{i,j}}{\Delta y}\right) \text{ and } F_{i,j-1/2} = D_{i,j-1/2}\left(\frac{p_{i,j}-p_{i,j-1}}{\Delta y}\right) \quad (3.1)$$

and

$$K_{i,j} = \frac{1}{\Delta x\Delta y}\int_{\Omega_{i,j}} K dx dy$$
$$Q_{i,j} = \int_{\Omega_{i,j}} Q\delta(x-x_i)\delta(y-y_j) dx dy$$

For interior elements, $K_{i,j}=1$. In the case of a tip element located, for example, as depicted in figure 3.1, we have $0<K_{i,j}<1$, with $K_{i,j}$ equal to the fraction that the tip element occupies in the rectangular parent element located at (i,j), i.e., the "fill" fraction $h_{i,j+1/2}h_{i-1/2,j}/2\Delta x\Delta y$ (see figure 3.1). For elements and their W, E, S, and N neighbors located at totally interior locations these equations reduce to the standard generalized finite difference equation system given by:

$$1\Delta x\Delta y\left(\frac{w_{i,j}-(w_{old})_{i,j}}{\Delta t}\right) - Q_{i,j} = \Delta y(F_{i+1/2,j}-F_{i-1/2,j})+ \\ \Delta x(F_{i,j+1/2}-F_{i,j-1/2}) \\ = \Delta y D_{i+1/2,j}\left(\frac{p_{i+1,j}-p_{i,j}}{\Delta x}\right)+ \\ \Delta y D_{i-1/2,j}\left(\frac{p_{i-1,j}-p_{i,j}}{\Delta x}\right)+ \\ \Delta x D_{i,j-1/2}\left(\frac{p_{i,j-1}-p_{i,j}}{\Delta y}\right)+ \\ \Delta x D_{i,j+1/2}\left(\frac{p_{i,j+1}-p_{i,j}}{\Delta y}\right) \\ = A_{i-\frac{1}{2},j}p_{i-1,j} + A_{i+\frac{1}{2},j}p_{i+1,j}+ \\ A_{i,j-\frac{1}{2}}p_{i,j-1} + A_{i,j+\frac{1}{2}}p_{i,j+1} + A_{i,j}p_{i,j}$$

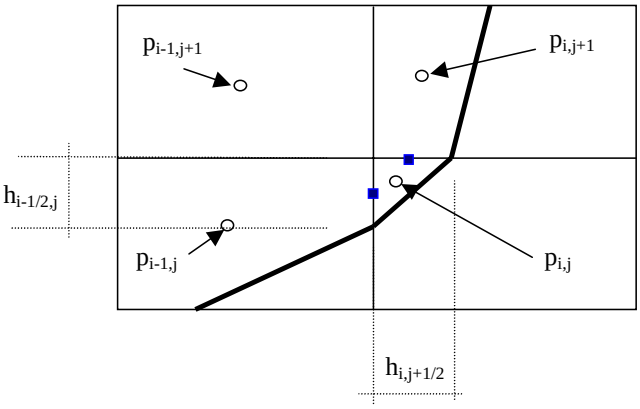

FIG. 3.1. *Finite Volume tip element collocation points*

where $A_{i,j} = -(A_{i-\frac{1}{2},j} + A_{i+\frac{1}{2},j} + A_{i,j-\frac{1}{2}} + A_{i,j+\frac{1}{2}})$, and

$$A_{i-\frac{1}{2},j} = \Delta y \frac{D_{i-\frac{1}{2},j}}{\Delta x},\ A_{i+\frac{1}{2},j} = \Delta y \frac{D_{i+\frac{1}{2},j}}{\Delta x},$$
$$A_{i,j-\frac{1}{2}} = \Delta x \frac{D_{i,j-\frac{1}{2}}}{\Delta y},\ A_{i,j+\frac{1}{2}} = \Delta x \frac{D_{i,j+\frac{1}{2}}}{\Delta y}$$

In the case of tip elements, we require pressure gradient information based on non-uniform element centroid locations. We thus assume that the pressure has the bilinear form $p(x,y) = ax + by + cxy + d$, where constants a, b, c, and d are to be determined from the four nearest neighbors, i.e., $p_{i-1,j}$, $p_{i,j}$, $p_{i,j+1}$, and $p_{i-1,j+1}$ in the case of figure 3.1. We require pressure derivatives for the flux calculations in (3.1), given by

$$\widehat{p}_x = a + cy$$
$$\widehat{p}_y = b + cx$$

where $\widehat{p}$ is collocated at the center of an edge of a tip element (marked by solid squares in figure 3.1). The fluxes are adjusted according to the edge lengths as follows:

$$\begin{aligned} F_{i-1/2,j} &= \frac{h_{i-1/2,j}}{\Delta y} \widehat{F}_{i-1/2,j} \\ &= \frac{h_{i-1/2,j}}{\Delta y} \widehat{D}_{i-1/2,j} (\widehat{p}_x)_{i-1/2,j} \end{aligned}$$

$$\begin{aligned} F_{i,j+1/2} &= \frac{h_{i,j+1/2}}{\Delta x} \widehat{F}_{i,j+1/2} \\ &= \frac{h_{i,j+1/2}}{\Delta x} \widehat{D}_{i,j+1/2} (\widehat{p}_y)_{i,j+1/2} \end{aligned}$$

Notice that, since we have a zero flux boundary condition imposed, the edge of partial element (i,j) that runs along the fracture perimeter provides a zero contribution to

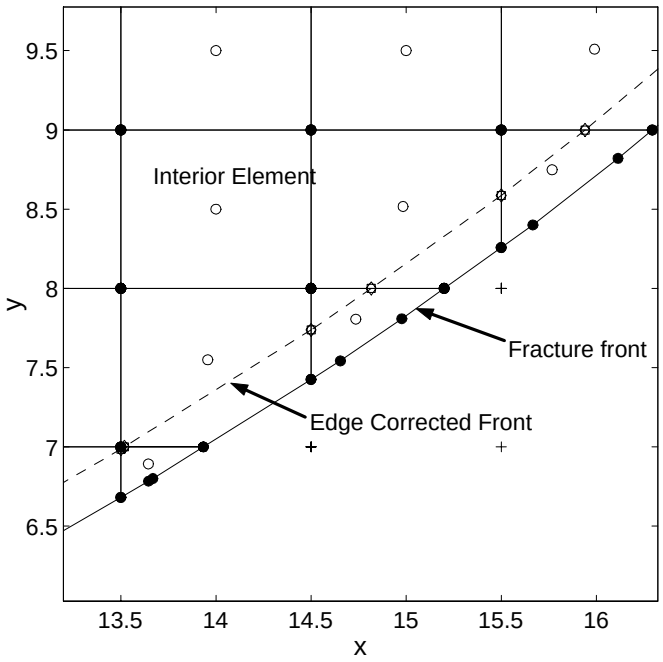

FIG. 3.2. *A portion of the Finite Volume Discretization of the fracture. Rectangular interior elements and polygonal tip elements are shown. The element certroids are denoted by ∘ symbols and the edge corrected front for the enhanced elasticty solution is shown.*

the equation system leaving only the above two flux contributions for the tip element as depicted in figure 3.1.

3.2. Discretization of the boundary integral equation. For the discretization of the elastic integral equation (2.1) we assume that the width is piece-wise constant over each element and collocate at the element centers. In this case the discrete elasticity equations assume the form:

$$Cw = p - \sigma_c \tag{3.2}$$

In the case of an inhomogeneous elastic medium the discretized collocation operator C is not symmetric. The procedure for constructing the Green's functions for layered elastic materials both in plane strain and in three dimensions is described in [4] and [5]. In order to enhance the accuracy of this discretization procedure we make use of the concept of partially fractured tip elements (see [6]) and a so-called edge-corrected front.

Figure 3.2 shows a typical meshing pattern near the tip of a typical hydraulic fracture for the Finite Volume approach. Indicated in the figure is the actual fracture front location as well as the edge-corrected fracture front, used to generate the elasticity influence coefficients. The small solid circles indicate polygon vertices, and the centroids of the elements are denoted by open circles.

4. Numerical Results. In this section, we provide hydraulic fracture growth results obtained using the Finite Volume approach with front-tracking, and a zero

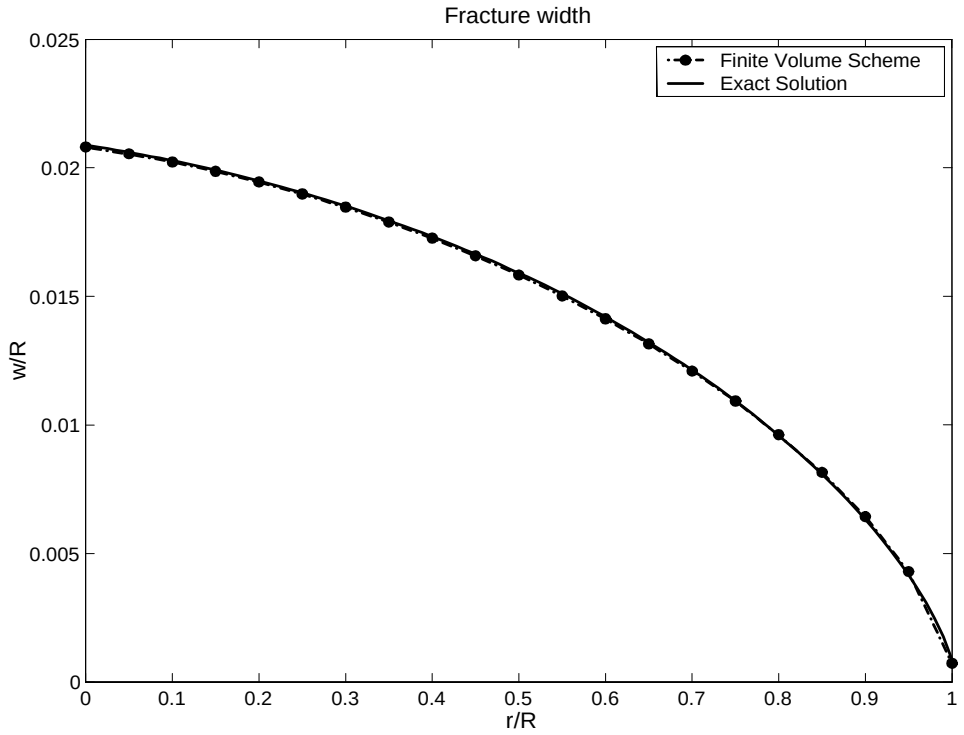

FIG. 4.1. *The normalized exact and Finite Volume numerical solutions for the fracture width profile w/R as a function of the dimensionless radius r/R for a radially symmetric penny-shaped fracture. The fracture radius at this stage in the evolution of the fracture is $R = 20m$.*

flux boundary condition at the fracture tip. The results are compared to the exact solution for a radial penny-shaped fracture [7]. For the comparison we have used the following input data: $E = 22\ kPa$, $\nu = 0.25$, $Q = 1\ m^3/s$, $\mu = 1\ Pa.s$, $\Delta x = \Delta y = 1\ m$. In figure 4.1 we compare the fracture width profile obtained using the Finite Volume scheme with the exact solution. There is excellent agreement between the two solutions. In figure 4.2 we compare the fluid pressure profile obtained using the Finite Volume scheme with the exact solution. Inside the fracture (not including the source point at which the pressure field has a logarithmic singularity) the agreement between the two solutions is very close.

However, close to the tip, where the pressure field has a singularity of order $O((R(t) - r)^{-\frac{1}{3}})$, the agreement between the solutions is not as good. In order to improve on the numerical solution in the vicinity of this singularity it would be necessary to build the shape function of this singularity into the Finite Volume formulation explicitly.

5. Conclusions. In this paper we have presented a novel Eulerian Finite Volume algorithm to solve the nonlinear coupled integro-partial differential equations describing a fluid-driven fracture in an elastic medium. In order to avoid having to reconstruct the Green's function matrix for the integral equation at each fracture footprint, which can be computationally intensive for a layered elastic material, it is necessary to consider a grid of rectangular elements that is set up *a priori* on which the hydraulic fracture is assumed to evolve. The coefficients of the Green's function

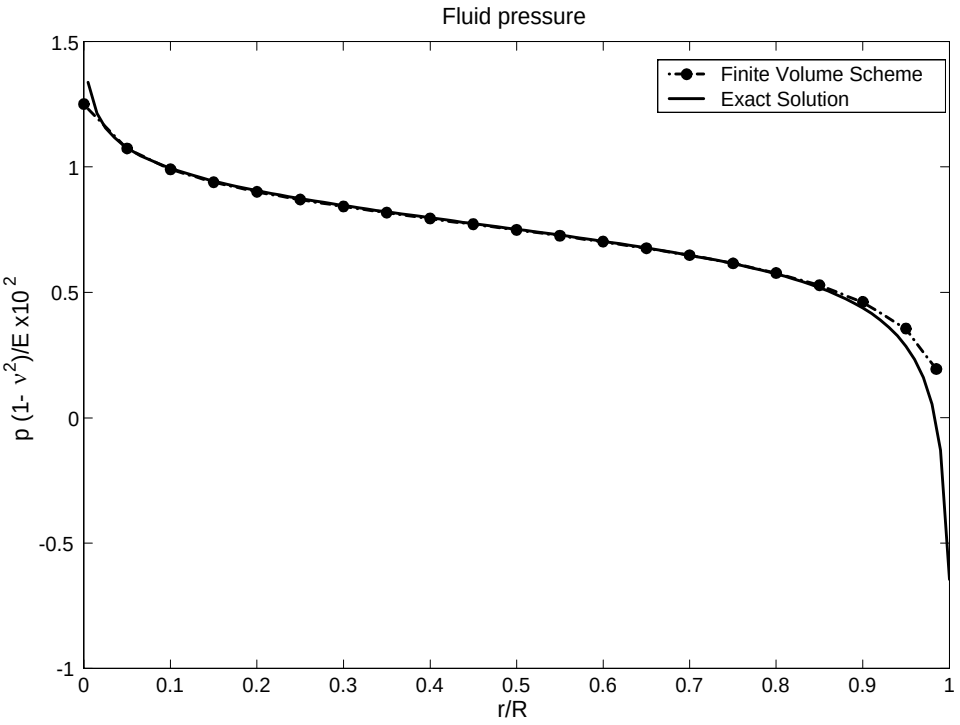

FIG. 4.2. *The normalized exact and Finite Volume numerical solutions for the fluid pressure field* $\frac{(1-\nu^2)}{E}p \times 100$ *as a function of the dimensionless radius* r/R *for a radially symmetric penny-shaped fracture. The fracture radius at this stage in the evolution of the fracture is* $R = 20m$.

can be pre-calculated for these rectangular elements, while the integral equation for the arbitrarily shaped fracture can be approximated accurately on this Cartesian grid using the edge-corrected element concept [6]. The Cartesian Finite Volume method [1] is used to provide an accurate description of the arbitrarily shaped fracture on elements defined on this rectangular grid. In the numerical comparison with the exact solution for a radially symmetric penny-shaped fracture the Finite Volume algorithm produces fracture width profiles that show close agreement with the exact solution. The pressure field provided by the Finite Volume algorithm also shows close agreement with the exact solution in regions where the pressure is regular, however close to the singularities in the pressure field there is some deviation from the exact solution. In order to remedy this situation, it will be necessary to incorporate shape functions into the Finite Volume scheme that build in the singularity explicitly.

Acknowledgements:
The authors would like to thank Schlumberger for permission to publish. The first author whishes to acknowledge the support of NSERC for his research programme.

REFERENCES

[1] Calhoun, D. and LeVeque, R.J., "A Cartesian grid finite-volume method for the advection-diffusion equation in irregular geometries", *J. Computat. Phys.*, **157**, 143-180, 2000.
[2] Clifton, R.J., and A.S. Abou-Sayed, "On the Computation of the Three-Dimensional Geometry of Hydraulic Fractures", SPE 7993, presented at the SPE/DOE Symposium of Low-Permeability Gas Reservoirs, Denver, CO., 1979.
[3] Clifton, J.R., "Three-Dimensional Hydraulic Fracturing", *SPE Monograph*, 1989.
[4] Peirce, A.P. and Siebrits, E., "Uniform asymptotic approximations for accurate modeling of cracks in layered elastic media", *International Journal of Fracture*, **110**, 205-239, 2001.
[5] Peirce, A.P. and Siebrits, E., "The scaled flexibility matrix method for the efficient solution of boundary value problems in 2D and 3D layered elastic media", *Computer methods in applied mechanics and engineering*, **190**, 5935-5956, 2001.
[6] Ryder, J.A. and Napier, J.A.L. (1985). Error analysis and design of a large-scale tabular mining stress analyzer, *Proceedings 5th International Conference of Numerical Methods in Geomechanics*, Nagoya, 1549–1555.
[7] Savitski, A. and Detournay, E., "Propagation of a penny-shaped fluid-driven fracture in an impermeable rock: asymptotic solutions", *International Journal of Solids and Structures*, Vol. 39, No. 26, pp 6311-6337, 2002.